Performance Comparison of Several Nonlinear Multi-Bernoulli Filters for Multi-Target Filtering

Meiqin Liu, Tongyang Jiang, Xie Wang, and Senlin Zhang
Dept. of Systems Science and Engineering
College of Electrical Engineering, Zhejiang University
Hangzhou 310027, P. R. China
Email: {liumeiqin,jiangtongyang,wangxiek,slzhang}@zju.edu.cn

***Abstract*—In this paper, the performance of four nonlinear multi-Bernoulli (MB) filters for multi-target filtering is compared in the presence of clutter and detection uncertainty. The filters under consideration are the extended Kalman (EK) Gaussian mixture (GM) MB filter, the unscented Kalman (UK) GM-MB filter, the cubature Kalman (CK) GM-MB filter, and the sequential Monte Carlo (SMC) MB filter. Monte Carlo (MC) analyses are presented for these four filters under different clutter density and different detection probability. Then these filters are evaluated in terms of both the Optimal Sub-Pattern Assignment (OSPA) distance and their respective computing time. Simulation results show that the CK-GM-MB filter is an attractive nonlinear MB filtering approach.**

I. Introduction

The random finite set (RFS) based multi-target filtering methods have attracted more attention in recent years. The finite set statistics (FISST) provides a rigorous Bayesian framework for multi-target filtering [1]. Since the optimal multi-target Bayes filter based on the RFS is generally intractable, some sub-optimal multi-target Bayes filters are proposed, such as the probability hypothesis density (PHD) filter based on the first order moment approximation [2], the cardinalized probability hypothesis density (CPHD) filter based on the RFS moment and cardinality approximations [3], and the multi-target multi-Bernoulli (MeMBer) filter based on the RFS density approximations [1]. Since the MeMBer filter overestimates the number of targets, Vo [4] improved the MeMBer filter and proposed the cardinality balanced Multi-target Multi-Bernoulli (CBMeMBer) filter which has an unbiased estimation in the number of targets. Both the Gaussian Mixture (GM) and sequential Monte Carlo (SMC) techniques have been implemented for the PHD, CPHD, and CBMeMBer filters [4],[5],[6],[7],[8]. The main advantage of the CBMeMBer filter is that each Bernoulli distribution represents one track and it's existence probability, so it allows reliable and inexpensive extraction of the target states in the SMC implementation. The SMC-CBMeMBer filter also outperforms the SMC-PHD and SMC-CPHD filters [4]. For the GM implementation, the GM-CBMeMBer filter shows the similar performance to the PHD filter.

Various implementations and extensions of the RFS-based multi-Bernoulli filter have been considered in [9],[10],[11],[12],[13],[14],[15]. The multi-Bernoulli filter has been applied to tracking from audio and video information [16], tracking in networks [17], tracking from image information [18],[19], and sensor management for multi-target tracking [20]. Hybrid multi-Bernoulli and Possion multi-target filters have been proposed in [21]. The CBMeMBer filter will be treated as the multi-Bernoulli (MB) filter throughout this paper.

The GM-MB filter has an analytical solution under linear Gaussian models, and can be extended to nonlinear models using the extended Kalman (EK) or unscented Kalman (UK) approximation. The SMC-MB filter can accommodate nonlinear and non-Gaussian models. The EK-GM-MB, UK-GM-MB, and SMC-MB filters have been implemented for nonlinear multi-target filtering [8]. However, the comprehensive comparison of these three multi-target filters for nonlinear models is not performed in [8]. Recently the cubature Kalman (CK) filter [22] which employs a third-degree spherical-radical cubature rule was proposed to handle the nonlinear models. Compared with the UK filter, the CK filter is more accurate and more principled in mathematical terms [22]. Therefore, in this paper, we study the joint usage of the CK approximation together with the GM-MB filter to hand the nonlinear multi-target filtering problem, and also compare its performance with the EK-GM-MB, UK-GM-MB, and SMC-MB filters under different scenarios. Then the Optimal Sub-Pattern Assignment (OSPA) distance [23] and the computing time are used to evaluate the performance of these four nonlinear MB filters.

The rest of this paper is organized as follows. Section II provides the background on the MB-RFS and MB recursion. The CK-GM-MB filter is studied in section III. In section IV, the EK-GM-MB, UK-GM-MB, CK-GM-MB, and SMC-MB filters are evaluated under different simulation conditions. Finally, the conclusion is draw in Section V.

II. Background

A. Multi-Bernoulli RFS

A Bernoulli RFS [4] has probability of $1-r$ of being empty, and probability r of being a singleton whose element is distributed according to a probability p. The probability density of a Bernoulli RFS X is given by

$$\pi(X) = \begin{cases} 1-r & X=\emptyset, \\ r\cdot p(x) & X=\{x\}. \end{cases} \tag{1}$$

An MB-RFS [4] is a union of a fixed number of independent Bernoulli RFS with existence probability $r^{(i)} \in (0,1)$ and probability density $p^{(i)}$,$i = 1, \cdots M$, where M is the number of Bernoulli RFS. Thus an MB-RFS is completely described by the MB parameter set $\{(r^{(i)}, p^{(i)})\}_{i=1}^{M}$. The probability density of an MB-RFS is given by

$$\pi(\emptyset) = \prod_{j=1}^{M} (1 - r^{(j)}) \tag{2}$$

and

$$\pi(\{x_1, \cdots, x_n\}) = \pi(\emptyset) \sum_{1 \leq i_1 \neq \cdots \neq i_n \leq M} \prod_{j=1}^{n} \frac{r^{(i_j)} p^{(i_j)}(x_j)}{1 - r^{(i_j)}}. \tag{3}$$

The probability density of an MB-RFS is abbreviated by $\pi = \{(r^{(i)}, p^{(i)})\}_{i=1}^{M}$ in this paper.

B. Multi-Target Bayes Filter

Under the RFS framework, all the target states and measurements are treated as the RFS. For example, suppose at time k, there are $N(k)$ target states $x_{k,1}, \cdots, x_{k,N(k)}$ and $M(k)$ measurements $z_{k,1}, \cdots, z_{k,M(k)}$. Under the RFS framework, the multi-target state set X_k and multi-target measurement set Z_k can be described as follows:

$$X_k = \{x_{k,1}, \cdots, x_{k,N(k)}\}$$
$$Z_k = \{z_{k,1}, \cdots, z_{k,M(k)}\}.$$

The multi-target Bayes filter propagates a multi-target probability distribution $\pi(\cdot|Z_{1:k})$ as follows:

$$\pi_{k|k-1}(X_k|Z_{1:k-1}) = \int f_{k|k-1}(X_k|X)\pi_{k-1}(X|Z_{1:k-1})\delta X \tag{4}$$

$$\pi_k(X_k|Z_{1:k}) = \frac{g_k(Z_k|X_k)\pi_{k|k-1}(X_k|Z_{1:k-1})}{\int g_k(Z_k|X)\pi_{k|k-1}(X|Z_{1:k-1})\delta X} \tag{5}$$

where the integrals in Eq. (4) and Eq. (5) are set integrals, $f_{k|k-1}(\cdot|\cdot)$ denotes the multi-target transition density and $g_k(\cdot|\cdot)$ denotes the multi-target likelihood.

C. The MB Recursion

The MB filter propagates the multi-target posterior density as an MB density recursively in time, given a sequence of measurements. The MB filter is a parameterized approximation to the multi-target Bayes filter. The MB recursion has been proposed in [4],[8], readers can refer to [4],[8] for details. The MB recursion is based on the following assumptions [4],[8]:

- Each target evolves and generates measurements independently.
- The birth targets are modeled as an MB-RFS and independent of the survival targets.
- The clutter is modeled as a Poisson RFS and independent of target-generated measurements.
- The posterior multi-target RFS is approximated as an MB-RFS.

Based on the above assumptions, the MB recursion can be summarized as follows.

The MB prediction: Assume at time $k-1$, the posterior multi-target density is an MB-RFS

$$\pi_{k-1} = \{(r_{k-1}^{(i)}, p_{k-1}^{(i)})\}_{i=1}^{M_{k-1}} \tag{6}$$

then the predicted multi-target density is also an MB-RFS, which can be described by

$$\pi_{k|k-1} = \{(r_{P,k|k-1}^{(i)}, p_{P,k|k-1}^{(i)})\}_{i=1}^{M_{k-1}} \cup \{(r_{\Gamma,k}^{(i)}, p_{\Gamma,k}^{(i)})\}_{i=1}^{M_{\Gamma,k}} \tag{7}$$

where

$$r_{P,k|k-1}^{(i)} = r_{k-1}^{(i)} \langle p_{k-1}^{(i)}, p_{S,k} \rangle \tag{8}$$

$$p_{P,k|k-1}^{(i)}(x) = \frac{\langle f_{k|k-1}(x|\cdot), p_{k-1}^{(i)} p_{S,k} \rangle}{\langle p_{k-1}^{(i)}, p_{S,k} \rangle} \tag{9}$$

$\langle \cdot, \cdot \rangle$ is the inner product defined between two real-valued functions α and β by $\langle \alpha, \beta \rangle = \int \alpha(x)\beta(x)dx$, $f_{k|k-1}(\cdot|\zeta)$ denotes a single target transition density given state ζ at time k, $p_{S,k}$ is the existence probability of a target at time k, and $\{(r_{\Gamma,k}^{(i)}, p_{\Gamma,k}^{(i)})\}_{i=1}^{M_{\Gamma,k}}$ are the parameters of the MB-RFS of birth targets at time k.

The MB update: Assume at time k, the predicted multi-target density is an MB-RFS

$$\pi_{k|k-1} = \{(r_{k|k-1}^{(i)}, p_{k|k-1}^{(i)})\}_{i=1}^{M_{k|k-1}} \tag{10}$$

then the posterior multi-target density is approximated by an MB-RFS

$$\pi_k = \{(r_{L,k}^{(i)}, p_{L,k}^{(i)})\}_{i=1}^{M_{k|k-1}} \cup \{(r_{U,k}(z), p_{U,k}(\cdot; z))\}_{z \in Z_k} \tag{11}$$

where

$$r_{L,k}^{(i)} = r_{k|k-1}^{(i)} \frac{1 - \langle p_{k|k-1}^{(i)}, p_{D,k} \rangle}{1 - r_{k|k-1}^{(i)} \langle p_{k|k-1}^{(i)}, p_{D,k} \rangle} \tag{12}$$

$$p_{L,k}^{(i)}(x) = p_{k|k-1}^{(i)}(x) \frac{1 - p_{D,k}(x)}{1 - \langle p_{k|k-1}^{(i)}, p_{D,k} \rangle} \tag{13}$$

$$r_{U,k}(z) = \frac{\sum_{i=1}^{M_{k|k-1}} \frac{r_{k|k-1}^{(i)}(1 - r_{k|k-1}^{(i)}) \langle p_{k|k-1}^{(i)}, \psi_{k,z} \rangle}{(1 - r_{k|k-1}^{(i)} \langle p_{k|k-1}^{(i)}, p_{D,k} \rangle)^2}}{\kappa_k(z) + \sum_{i=1}^{M_{k|k-1}} \frac{r_{k|k-1}^{(i)} \langle p_{k|k-1}^{(i)}, \psi_{k,z} \rangle}{1 - r_{k|k-1}^{(i)} \langle p_{k|k-1}^{(i)}, p_{D,k} \rangle}} \tag{14}$$

$$p_{U,k}(x; z) = \frac{\sum_{i=1}^{M_{k|k-1}} \frac{r_{k|k-1}^{(i)}}{1 - r_{k|k-1}^{(i)}} p_{k|k-1}^{(i)}(x) \psi_{k,z}(x)}{\sum_{i=1}^{M_{k|k-1}} \frac{r_{k|k-1}^{(i)}}{1 - r_{k|k-1}^{(i)}} \langle p_{k|k-1}^{(i)} \psi_{k,z} \rangle} \tag{15}$$

where $\psi(x) = g_k(z|x)p_{D,k}(x)$, Z_k is the measurement set at time k, $g_k(\cdot|x)$ is the single measurement likelihood given state x at time k, $p_{D,k}$ is the detection probability at time k, and $\kappa(\cdot)$ is the intensity of clutter at time k.

III. The CK-GM-MB Filter

In multi-target tracking, the motion and measurement models may be nonlinear. Although the EK-GM-CB, UK-GM-CB, and SMC-MB filters have been proposed for the nonlinear multi-target filtering, the comprehensive comparison is not performed in [4]. In this paper, we also study the joint usage of the CK approximation with the GM-MB filter for nonlinear multi-target filtering, and compare its performance with the EK-GM-CB, UK-GM-CB, and SMC-MB filters in terms of both the OSPA metric and their respective computing time under different clutter density and different detection probability.

A. The CK Approximation

Suppose each target follows a nonlinear motion and measurement model, i.e,

$$x_k = f(x_{k-1}) + w_{k-1} \tag{16}$$

$$z_k = h(x_k) + v_k \tag{17}$$

where $f(\cdot)$ and $h(\cdot)$ are the known nonlinear functions, w_{k-1} and v_k are independent zero mean Gaussian process noise and measurement noise with known covariances Q_{k-1} and R_k, respectively.

The key idea of the CK filtering algorithm is that it uses the third-degree spherical-radial rule to calculate a Gaussian weighted integral, which can be described as follows:

$$\int_{\mathbb{R}^n} f(x)\mathcal{N}(x;0,\mathrm{I})dx \approx \sum_{l=1}^{2n} \omega(l) f(\xi(l)) \tag{18}$$

where $\mathrm{I} \in \mathbb{N}^{n\times n}$ is the identity matrix, n is the dimension of the state x, $\xi(l)$ is the lth cubature point, $\omega(l)$ is the weight of the lth cubature point, $\omega(l) = \frac{1}{2n}$, and $\xi(l)$ is the lth column of Ψ.

$$\Psi = \sqrt{n}\left\{ \underbrace{\begin{pmatrix}1\\ \vdots\\ 0\end{pmatrix}, \cdots \begin{pmatrix}0\\ \vdots\\ 1\end{pmatrix}}_{n}, \underbrace{\begin{pmatrix}-1\\ \vdots\\ 0\end{pmatrix}, \cdots \begin{pmatrix}0\\ \vdots\\ -1\end{pmatrix}}_{n} \right\} \tag{19}$$

B. The CK-GM-MB Recursion

According to the CK approximation, the CK-GM-MB recursion can be derived easily. The CK-GM-MB recursion consists of the prediction and update.

Prediction: Assume at time $k-1$, the posterior multi-target density

$$\pi_{k-1} = \{(r_{k-1}^{(i)}, p_{k-1}^{(i)})\}_{i=1}^{M_{k-1}} \tag{20}$$

is given and each probability density $p_{k-1}^{(i)}$ is comprised of the Gaussian mixtures

$$p_{k-1}^{(i)}(x) = \sum_{j=1}^{J_{k-1}^{(i)}} w_{k-1}^{(i,j)} \mathcal{N}(x; m_{k-1}^{(i,j)}, P_{k-1}^{(i,j)}), \tag{21}$$

then the predicted multi-target density

$$\pi_{k|k-1} = \{(r_{P,k|k-1}^{(i)}, p_{P,k|k-1}^{(i)})\}_{i=1}^{M_{k-1}} \cup \{(r_{\Gamma,k}^{(i)}, p_{\Gamma,k}^{(i)})\}_{i=1}^{M_{\Gamma,k}} \tag{22}$$

can be computed as follows:

$$r_{P,k|k-1}^{(i)} = r_{k-1}^{(i)} p_{S,k}, \tag{23}$$

$$p_{P,k|k-1}^{(i)}(x) = \sum_{j=1}^{J_{k-1}^{(i)}} w_{k-1}^{(i,j)} \mathcal{N}(x; m_{P,k|k-1}^{(i,j)}, P_{P,k|k-1}^{(i,j)}) \tag{24}$$

where

$$C_{k-1}^{(i,j)} = \mathrm{chol}[P_{k-1}^{(i,j)}]^T \tag{25}$$

"chol" denotes the Cholesky decomposition,

$$\chi_{k-1}^{(i,j)}(l) = m_{k-1}^{(i,j)} + C_{k-1}^{(i,j)} \xi(l) \tag{26}$$

$l = 1, \cdots, 2n$, n is the dimension of state $m_{k-1}^{(i,j)}$, $\xi(l)$ is the lth column of Ψ, Ψ can be computed according to Eq. (19),

$$\chi_{k|k-1}^{(i,j)}(l) = f(\chi_{k-1}^{(i,j)}(l)) \tag{27}$$

$$m_{P,k|k-1}^{(i,j)} = \frac{1}{2n}\sum_{l=1}^{2n} \chi_{k|k-1}^{(i,j)}(l) \tag{28}$$

$$\begin{aligned} P_{P,k|k-1}^{(i,j)} &= Q_{k-1} + \\ &\frac{1}{2n}\sum_{l=1}^{2n} (m_{P,k|k-1}^{(i,j)} - \chi_{k|k-1}^{(i,j)}(l))(m_{P,k|k-1}^{(i,j)} - \chi_{k|k-1}^{(i,j)}(l))^T \end{aligned} \tag{29}$$

$\{(r_{\Gamma,k}^{(i)}, p_{\Gamma,k}^{(i)})\}_{i=1}^{M_{\Gamma,k}}$ are birth models, which can be described by the Gaussian mixtures [4].

Update: Assume at time k, the predicted multi-target density

$$\pi_{k|k-1} = \{(r_{k|k-1}^{(i)}, p_{k|k-1}^{(i)})\}_{i=1}^{M_{k|k-1}} \tag{30}$$

is given and each probability $p_{k|k-1}^{(i)}$ is comprised of the Gaussian mixtures

$$p_{k|k-1}^{(i)}(x) = \sum_{j=1}^{J_{k|k-1}^{(i)}} w_{k|k-1}^{(i,j)} \mathcal{N}(x; m_{k|k-1}^{(i,j)}, P_{k|k-1}^{(i,j)}), \tag{31}$$

then the updated density

$$\pi_k = \{(r_{L,k}^{(i)}, p_{L,k}^{(i)})\}_{i=1}^{M_{k|k-1}} \cup \{(r_{U,k}(z), p_{U,k}(\cdot; z))\}_{z\in Z_k} \tag{32}$$

can be computed as follows:

$$r_{L,k}^{(i)} = r_{k|k-1}^{(i)} \frac{1 - p_{D,k}}{1 - r_{k|k-1}^{(i)} p_{D,k}} \tag{33}$$

$$p_{L,k}^{(i)}(x) = p_{k|k-1}^{(i)}(x) \tag{34}$$

$$r_{U,k}(z) = \frac{\sum_{i=1}^{M_{k|k-1}} \frac{r_{k|k-1}^{(i)}(1-r_{k|k-1}^{(i)})\varrho_{U,k}^{(i)}(z)}{(1-r_{k|k-1}^{(i)} p_{D,k})^2}}{\kappa_k(z) + \sum_{i=1}^{M_{k|k-1}} \frac{r_{k|k-1}^{(i)} \varrho_{U,k}^{(i)}(z)}{1-r_{k|k-1}^{(i)} p_{D,k}}} \tag{35}$$

$$p_{U,k}(\cdot;z) = \frac{\sum_{i=1}^{M_{k|k-1}} \sum_{j=1}^{J_{k|k-1}^{(i)}} w_{U,k}^{(i,j)}(z)\mathcal{N}(x; m_{U,k}^{(i,j)}, P_{U,k}^{(i,j)})}{\sum_{i=1}^{M_{k|k-1}} \sum_{j=1}^{J_{k|k-1}^{(i)}} w_{U,k}^{(i,j)}(z)} \tag{36}$$

where

$$\varrho_{U,k}^{(i)}(z) = p_{D,k}\Sigma_{j=1}^{J_{k|k-1}^{(i)}} w_{k|k-1}^{(i,j)} q_k^{(i,j)}(z) \tag{37}$$

$$q_k^{(i,j)}(z) = \mathcal{N}(z; \eta_{U,k|k-1}^{(i,j)}, S_{U,k}^{(i,j)}) \tag{38}$$

$$w_{U,k}^{(i,j)}(z) = \frac{r_{k|k-1}^{(i)}}{1 - r_{k|k-1}^{(i)}} P_{D,k} w_{k|k-1}^{(i,j)} q_k^{(i,j)}(z) \tag{39}$$

$$C_{k|k-1}^{(i,j)} = \text{chol}[P_{k|k-1}^{(i,j)}]^T \tag{40}$$

$$\chi_{k|k-1}^{(i,j)}(l) = m_{k|k-1}^{(i,j)} + C_{k|k-1}^{(i,j)}\xi(l) \tag{41}$$

$$z_{k|k-1}^{(i,j)}(l) = h(\chi_{k|k-1}^{(i,j)}(l)) \tag{42}$$

$$\eta_{U,k|k-1}^{(i,j)} = \frac{1}{2n}\sum_{l=1}^{2n} z_{k|k-1}^{(i,j)}(l) \tag{43}$$

$$S_{U,k}^{(i,j)} = \frac{1}{2n}\sum_{l=1}^{2n}(\eta_{U,k|k-1}^{(i,j)} - z_{k|k-1}^{(i,j)}(l))(\eta_{U,k|k-1}^{(i,j)} - z_{k|k-1}^{(i,j)}(l))^T + R_k \tag{44}$$

$$G_{U,k}^{(i,j)} = \frac{1}{2n}\sum_{l=1}^{2n}(m_{k|k-1}^{(i,j)} - \chi_{k|k-1}^{(i,j)}(l))(\eta_{U,k|k-1}^{(i,j)} - z_{k|k-1}^{(i,j)}(l))^T \tag{45}$$

$$K_{U,k}^{(i,j)} = G_{U,k}^{(i,j)}[S_{U,k}^{(i,j)}]^{-1} \tag{46}$$

$$m_{U,k}^{(i,j)} = m_{k|k-1}^{(i,j)} + K_{U,k}^{(i,j)}(z - \eta_{U,k|k-1}^{(i,j)}) \tag{47}$$

$$P_{U,k}^{(i,j)} = P_{k|k-1}^{(i,j)} - K_{U,k}^{(i,j)} S_{U,k}^{(i,j)} [K_{U,k}^{(i,j)}]^T \tag{48}$$

Remark 1. It's noted that the CK-GM-MB recursion is similar to the UK-GM-MB recursion, the main difference is the choice of the sigma points. The UK-GM-MB filter needs $2n+1$ sigma points at each recursion, while the CK-GM-MB filter needs $2n$ sigma points.

The multi-target state can be estimated by two steps [4]. First, estimate the number of targets from the posterior distribution of cardinality. Second, select the relevant number of hypothesized tracks with the highest existence probabilities, and estimate the state from each posterior track density using either the expected a posterior (EAP) or maximum a posterior (MAP) approach.

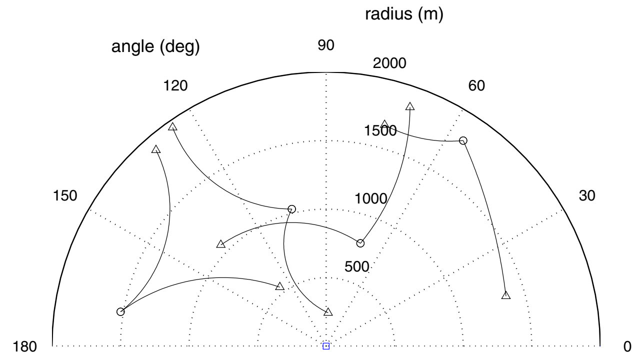

Fig. 1. True target tracks in $r\theta$ plane (the start/end positions for each track are denoted by $\circ/\triangle$, and the sensor is denoted by $\square$).

IV. Simulation Results

A. Simulation Scenario

Consider the noisy bearings and range measurements with varying number of targets observed in clutter environments. The surveillance region size is $[0, \pi]$ rad $\times$ $[0, 2000]$ m. A maximum of 8 targets appears on the scenario, and targets appear and terminate randomly. The true tracks are shown in Fig. 1.

The motion dynamics is a coordinated turn (CT) model, which is described by

$$x_k = F(\omega_{k-1})x_{k-1} + Gw_{k-1}, \tag{49}$$

$$F(\omega_{k-1}) = \begin{bmatrix} 1 & \frac{\sin\omega_{k-1}T}{\omega_{k-1}} & 0 & -\frac{1-\cos\omega_{k-1}T}{\omega_{k-1}} & 0 \\ 0 & \cos\omega_{k-1}T & 0 & -\sin\omega_{k-1}T & 0 \\ 0 & \frac{1-\cos\omega_{k-1}T}{\omega_{k-1}} & 1 & \frac{\sin\omega_{k-1}T}{\omega_{k-1}} & 0 \\ 0 & \sin\omega_{k-1}T & 0 & \cos\omega_{k-1}T & 0 \\ 0 & 0 & 0 & 0 & 1 \end{bmatrix}, \tag{50}$$

$$G = \begin{bmatrix} \frac{T^2}{2} & 0 & 0 \\ T & 0 & 0 \\ 0 & \frac{T^2}{2} & 0 \\ 0 & T & 0 \\ 0 & 0 & T \end{bmatrix}, \tag{51}$$

where T is the sampling period, $T = 1$ s, $w_{k-1} \sim \mathcal{N}(\cdot; 0, Q_{k-1})$, the noise covariance matrix is $Q_{k-1} = \text{diag}([\sigma_w^2, \sigma_w^2, \sigma_\omega^2]^T)$, $\sigma_w = 5$ m/s^2 and $\sigma_\omega = (\pi/180)$ rad/s. The target state $x_k = [p_{x,k}, \dot{p}_{x,k}, p_{y,k}, \dot{p}_{y,k}, \omega_k]^T$ consists of the position $(p_{x,k}, p_{y,k})$, velocity $(\dot{p}_{x,k}, \dot{p}_{y,k})$, and turn rate ω_k.

The measurement is the noisy bearing and range model [5], which is described by

$$z_k = \begin{bmatrix} \arctan[(p_{x,k} - p_{Se,x})/(p_{y,k} - p_{Se,y})] \\ \sqrt{(p_{x,k} - p_{Se,x})^2 + (p_{y,k} - p_{Se,y})^2} \end{bmatrix} + v_k, \tag{52}$$

where $(p_{Se,x}, p_{Se,y}) = (0, 0)$ is the sensor position, $v_k \sim \mathcal{N}(\cdot; 0, R_k)$ with $R_k = \text{diag}([\sigma_\theta^2, \sigma_r^2]^T)$, $\sigma_\theta = 1 \times (\pi/180)$ rad/s, and $\sigma_r = 10$ m.

The birth process is an MB-RFS with density

$$\pi_\Gamma = \{(r_\Gamma^{(i)}, p_\Gamma^{(i)})\}_{i=1}^4,$$

where

$$r_\Gamma^{(i)} = 0.03,$$
$$p_\Gamma^{(i)} = \mathcal{N}(x; m_\Gamma^{(i)}, P_\Gamma^{(i)}),$$
$$m_\Gamma^{(1)} = [-1500, 0, 250, 0, 0]^T,$$
$$m_\Gamma^{(2)} = [-250, 0, 1000, 0, 0]^T,$$
$$m_\Gamma^{(3)} = [250, 0, 750, 0, 0]^T,$$
$$m_\Gamma^{(4)} = [1000, 0, 1500, 0, 0]^T,$$
$$P_\Gamma^{(i)} = \text{diag}([10, 10, 10, 10, 1 \times (\pi/180)]^T)^2.$$

The survival probability is $p_{S,k} = 0.99$. The detection probability is $p_{D,k} = 0.98$.

Clutter is modeled as a Poisson RFS K_k with intensity [5]

$$\kappa_k = \lambda_c V u(z), \tag{53}$$

where λ_c is the average number of clutter measurements per scan, and $u(z)$ is the uniform density over the surveillance region. The clutter density is $\lambda_c = 1.6 \times 10^{-3}(\text{radm})^{-1}$ (an average of 10 clutter measurements per scan).

In the GM/SMC implementation of nonlinear multi-Bernoulli filters, as the number of GM components/particles required to represent the multi-target density increases without bound, the pruning strategies are needed to limit the number of GM components/particles [4],[5]. In the GM implementation, pruning of hypothesized tracks is performed with weight threshold of $T_r = 10^{-4}$. Pruning and merging of Gaussian components are also performed at each time. The pruning threshold is $T^{'} = 10^{-5}$. The merging threshold is $U^{'} = 4$. The maximum of Gaussian components for each hypothesized track is $J_{\max} = 100$. In the SMC implementation, a maximum of 100 and minimum of 50 particles for each hypothesized track is imposed. Pruning of hypothesized tracks is performed with a threshold of 10^{-4} and a maximum of 100 tracks.

B. Metrics for Multi-Target Filtering

To evaluate the performance of the above four nonlinear MB filters, the OSPA metric [23] is considered in this paper. The OSPA distance can jointly capture difference in cardinality and individual elements between two finite sets in a mathematically consistent yet intuitively meaningful way. The OSPA metric $\bar{d}_p^{(c)}$ is defined as follows. Let $d^{(c)}(x,y) := \min(c, ||x-y||)$ denote the distance between x, y cut off at $c > 0$, and Π_k denote the set of permutations on $\{1, 2 \cdots, k\}$ for any $k \in \{1, 2, \cdots\}$, where $||\cdot||$ is the Euclidean norm. For $1 \le p \le \infty$, $c > 0$, and arbitrary finite subsets $X = \{x_1, \cdots, x_m\}$ and $Y = \{y_1, \cdots, y_n\}$, where $m, n \in \{0, 1, 2, \cdots\}$, define

$$\bar{d}_p^{(c)}(X,Y) := \left(\frac{1}{n}\left(\min_{\pi\in\Pi_n}\sum_{i=1}^{m} d^{(c)}(x_i, y_{\pi(i)})^p + c^p(n-m)\right)\right)^{\frac{1}{p}} \tag{54}$$

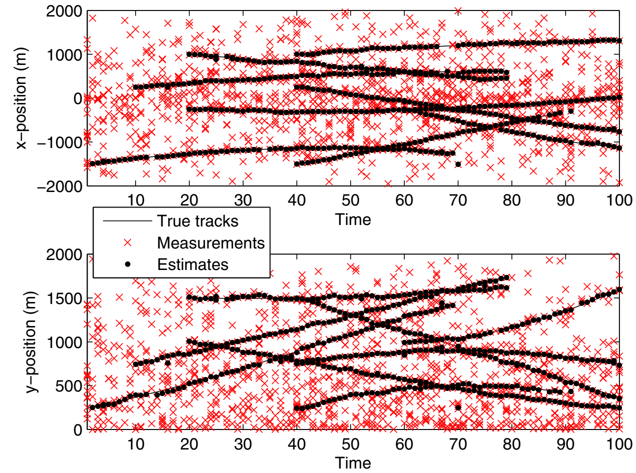

Fig. 2. True target tracks, measurements and estimates in x and y directions versus time for the CK-GM-MB filter.

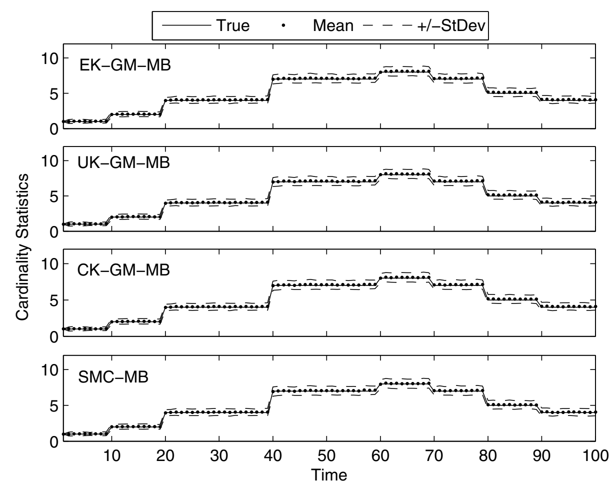

Fig. 3. The 500 MC run averages of cardinality statistics versus time for the EK-GM-MB, UK-GM-MB, CK-GM-MB, and SMC-MB filters.

if $m \le n$, and $\bar{d}_p^{(c)}(X,Y) = \bar{d}_p^{(c)}(Y,X)$, if $m > n$; and $\bar{d}_p^{(c)}(X,Y) = \bar{d}_p^{(c)}(Y,X) = 0$ if $m = n = 0$. The order parameter p determines the sensitivity to outliers, and the cut-off parameter c determines the relative weighting of the penalties assigned to cardinality and localization errors.

C. Monte Carlo Runs

To compare the performance of the EK-GM-MB, UK-GM-MB, CK-GM-MB, and SMC-MB filters, 500 Monte Carlo trails are performed on the same target tracks but with randomly generated measurements data.

Fig. 2 plots the true tracks, measurements, and estimates in x and y directions versus time for the CK-GM-MB filter. The plots show that the CK-GM-MB filter is also able to estimate the true tracks of the multi-target. In Fig. 3 the averages and standard deviation of the cardinality statistics for the EK-GM-MB, UK-GM-MB, CK-GM-MB, and SMC-

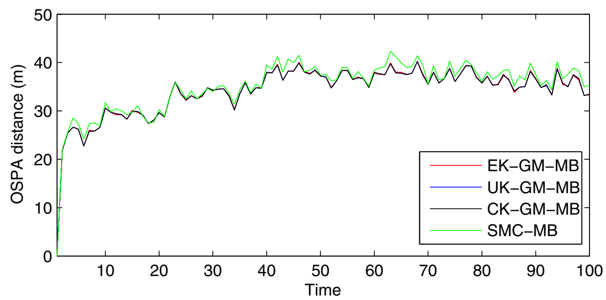

Fig. 4. The 500 MC averages of OSPA distance for the EK-GM-MB, UK-GM-MB, CK-GM-MB, and SMC-MB filters.

TABLE I
COMPARISON OF FOUR NONLINEAR MB FILTERS

Algorithm	Time av. OSPA (m)	Av. comput. time (s)
EK-GM-MB	34.1346	7.06
UK-GM-MB	34.1296	15.74
CK-GM-MB	34.1287	14.87
SMC-MB	35.0623	118.57

MB filters are shown versus time. It can be seen that the averages of the cardinality statistics for the EK-GM-MB, UK-GM-MB, CK-GM-MB, and SMC-MB filters converge to the true value. Fig. 3 also shows that the EK-GM-MB, UK-GM-MB, CK-GM-MB, and SMC-MB filters almost have the same standard deviation of the cardinality statistics. We can hardly see the obvious difference in both the averages and standard deviation of the cardinality statistics from Fig. 3. The 500 MC averages of OSPA distance (for p=2 and c=200) for the EK-GM-MB, UK-GM-MB, CK-GM-MB, and SMC-MB filters are plotted in Fig.4. As shown in Fig. 4, the curves of the EK-GM-MB, UK-GM-MB, and CK-GM-MB filters are almost overlapped. This indicates that the EK-GM-MB, UK-GM-MB, and CK-GM-MB filters have the similar filtering accuracy. The filtering accuracy of the SMC-MB filter is the worst, because the number of particles for each hypothesized track is not enough. The SMC-MB filter is the optimal nonlinear MB filtering approach. When the number of the particles for each hypothesized track is large enough, the SMC-MB filtering approach will get the best filtering accuracy. Meanwhile, a large number of particles means a large amount of calculation, which will limit the real-time performance of the MB filtering.

Table I gives the 500 MC time average OSPA distance and the 500 MC average computing time in MATLAB R2011a on a notebook with clutter density $\lambda_c = 1.6 \times 10^{-3}$ (radm)$^{-1}$ (an average of 10 clutter measurements per scan). From Table I we can see that, the time average OSPA distance of the EK-GM-MB, UK-GM-MB, and CK-GM-MB filters is close, the best is the CK-GM-MB filter, the second is the UK-GM-MB filter, the third is the EK-GM-MB filter, and the worst is the SMC-MB filter. The OSPA distance of the EK-GM-MB, UK-GM-MB, and CK-GM-MB filters is close, most likely because the motion and measurement models are mildly nonlinear. Table I also shows that, the EK-GM-MB filter has the best real-time performance. The real-time performance of the CK-GM-MB filter is superior to the UK-GM-MB filter, because the CK-GM-MB filter only needs $2n$ sigma points to approximate the first and second moment of the probability density, while the UK-GM-MB filter needs $2n + 1$ sigma points. The real-time performance of the SMC-MB filter is the worst, because the SMC-MB filtering algorithm needs a large number of the particles. Therefore, in view of both the filtering performance and the real-time performance, the CK-GM-MB filter is an attractive approach.

Remark 2. Similar to the single target filtering, the EK-GM-MB filter is only applied to the continuous and differentiable nonlinear models. Sometimes, even if the nonlinear motion and measurement models are differentiable, computing the Jacobian matrices may be hard. The UK-GM-MB and CK-GM-MB filters are able to overcome the above problems. Compared with the UK-GM-MB filter, the CK-GM-MB filter has a better real-time performance.

Remark 3. When the motion and measurement models are highly nonlinear, the SMC-MB filter is an attractive method.

To evaluate the performance of these four nonlinear MB filters further, 500 MC trails are performed over varying clutter density from $\lambda_c = 0$ (radm)$^{-1}$ to $\lambda_c = 3.2 \times 10^{-3}$ (radm)$^{-1}$ (from an average of 0 clutter measurement to 20 clutter measurements per scan) and varying detection probability from $p_{D,k} = 0.90$ to $p_{D,k} = 1$.

Table II gives the performance comparison of four nonlinear MB filters under varying clutter density. From Table II we can see that the time average OSPA distance of the EK-GM-MB, UK-GM-MB, and CK-GM-MB filters is also close under different clutter density. The CK-GM-MB filter shows almost the same filtering accuracy to the UK-GM-MB filter, and the CK-GM-MB filter is not always superior to the UK-GM-MB filter. The filtering accuracy of the CK-GM-MB and UK-GM-MB filters is slightly superior to the EK-GM-MB filter, and the SMC-MB filter is the worst. These four approaches in the order of the real-time performance are the EK-GM-MB filter, the CK-GM-MB filter, the UK-GM-MB filter, and the SMC-MB filter.

Table III gives the performance comparison of four nonlinear MB filters under varying detection probability. From Table III we can see that the time average OSPA distance of the EK-GM-MB, UK-GM-MB, and CK-GM-MB filters is still close under different detection probability, and the CK-GM-MB and UK-GM-MB filters are slightly superior to the EK-GM-MB filter, too. These four approaches in the order of the real-time performance are the EK-GM-MB filter, the CK-GM-MB filter, the UK-GM-MB filter and the SMC-MB filter, too.

Therefore, when the motion and measurement models are not highly nonlinear, in view of both the filtering performance and the real-time performance, the CK-GM-MB filter is an attractive nonlinear MB filtering approach.

V. CONCLUSION

We have compared the performance of the EK-GM-MB, UK-GM-MB, CK-GM-MB, and SMC-MB filters for nonlinear multi-target filtering. The MC simulation results show that the

TABLE II
PERFORMANCE COMPARISON OF FOUR NONLINEAR MB FILTERS UNDER VARYING CLUTTER DENSITY

Algorithm	0 clutter		5 clutter		15 clutter		20 clutter	
	Time av. OSPA (m)	Av. comput. time (s)	Time av. OSPA (m)	Av. comput. time (s)	Time av. OSPA (m)	Av. comput. time (s)	Time av. OSPA (m)	Av. comput. time (s)
EK-GM-MB	23.5492	3.09	29.6360	4.38	37.7132	8.27	40.8988	11.95
UK-GM-MB	23.5394	6.40	29.6310	9.69	37.6874	18.64	40.8934	27.82
CK-GM-MB	23.5390	6.09	29.6287	9.17	37.6866	17.81	40.8942	26.43
SMC-MB	24.7396	46.29	30.8193	72.42	38.3839	141.38	41.2704	200.67

TABLE III
PERFORMANCE COMPARISON OF FOUR NONLINEAR MB FILTERS UNDER VARYING DETECTION PROBABILITY

Algorithm	$p_{D,k} = 0.90$		$p_{D,k} = 0.94$		$p_{D,k} = 0.96$		$p_{D,k} = 1$	
	Time av. OSPA (m)	Av. comput. time (s)	Time av. OSPA (m)	Av. comput. time (s)	Time av. OSPA (m)	Av. comput. time (s)	Time av. OSPA (m)	Av. comput. time (s)
EK-GM-MB	55.6643	10.11	45.5281	9.07	39.4880	7.63	30.3923	2.55
UK-GM-MB	55.6534	22.78	45.5256	20.47	39.4666	17.40	30.3920	5.87
CK-GM-MB	55.6558	21.71	45.5252	19.39	39.4647	16.48	30.3893	5.53
SMC-MB	56.9919	151.28	46.6721	141.25	40.4267	123.99	29.8667	61.47

CK-GM-MB and UK-GM-MB filters have almost the same filtering accuracy. The filtering accuracy of the CK-GM-MB and UK-GM-MB filters is slightly superior to the EK-GM-MB filter, and the SMC-MB filter has the worst filtering accuracy since the number of the particles is not large enough. The EK-GM-MB filter has the best real-time performance, the second is the CK-GM-MB filter, the third is the UK-GM-MB filter, and the last is the SMC-MB filter. In view of both the filtering performance and the real-time performance, the CK-GM-MB filter is an attractive nonlinear MB filtering method.

ACKNOWLEDGMENT

This work was supported in part by the National Natural Science Foundation of China under Grants 61174142, 61222310, and 61374021, the Zhejiang Provincial Natural Science Foundation of China under Grants LZ14F030002 and LZ14F030003, the Specialized Research Fund for the Doctoral Program of Higher Education of China (SRFDP) under Grants 20120101110115 and 20130101110109, the Fundamental Research Funds for the Central Universities under Grant 2014XZZX003-12, the Open Fund for the Aircraft Marine Measurement and Control Joint Laboratory under Grant FOM2014OF06, and the ASFC under Grant 20132076002.

REFERENCES

[1] R. Mahler, *Statistical Multisource-Multitarget Information Fusion*. Norwood: Artech House, 2007.

[2] ——, "Multitarget Bayes filtering via first-order multitarget moments," *IEEE Trans. Aerosp. Electron. Syst.*, vol. 39, no. 4, pp. 1152–1178, Oct. 2003.

[3] ——, "PHD filters of higher order in target number," *IEEE Trans. Aerosp. Electron. Syst.*, vol. 43, no. 4, pp. 1523–1543, Oct. 2007.

[4] B.-T. Vo, B.-N. Vo, and A. Cantoni, "The cardinality balanced multi-target multi-Bernoulli filter and its implementations," *IEEE Trans. Signal Process.*, vol. 57, no. 2, pp. 409–423, Feb. 2009.

[5] B.-N. Vo, and W. Ma, "The Gaussian mixture probability hypothesis density filter," *IEEE Trans. Signal Process.*, vol. 54, no. 11, pp. 1091–4004, Nov. 2006.

[6] B.-N. Vo, S. Singh, and A. Doucet, "Sequential Monte carlo methods for multi-target filtering with random finite sets," *IEEE Trans. Aerosp. Electron. Syst.*, vol. 41, no. 4, pp. 1224–1245, Oct. 2005.

[7] B.-T. Vo, B.-N. Vo, and A. Cantoni, "Analytic implementations of the cardinalized probability hypothesis density filter," *IEEE Trans. Signal Process.*, vol. 55, no. 7, pp. 3553–3567, Jul. 2007.

[8] B.-T. Vo, "Random finite sets in multi-object filtering," Ph.D. dissertation, The University of Western Australia, Perth,Australia, Oct. 2008.

[9] B.-T. Vo, B.-N. Vo, R. Hoseinnezhad, and R. Mahler, "Multi-Bernoulli filtering with unknown clutter intensity and sensor field-of-view," in *in Proc. IEEE Conf. inf. Sci. Syst.*, Baltimore, MD, March 23-25, 2011, pp. 1–6.

[10] E. Baser, T. Kirubarajan, and M. Efe, "Improved MeMBer filter with modeling of spurious targets," in *Int. Conf. Inf. Fusion*, Istanbul, Turkey, Jul. 9-12, 2013, pp. 813–819.

[11] S. Reuter, D. Meissner, B. Wilking, and K. Dietmayer, "Cardinality balanced multi-target multi-Bernoulli filtering using adaptive birth distributions," in *Int. Conf. Inf. Fusion*, Istanbul, Turkey, Jul. 9-12, 2013, pp. 1608–1615.

[12] V.C. Ravindra, L. Svensson, L. Hammarstrand, and M. Morelande, "A cardinality preserving multitarget multi-Bernoulli RFS tracker," in *Int. Conf. Inf. Fusion*, Singapore, Jul. 9-12, 2012, pp. 832–839.

[13] B.-T. Vo, B.-N. Vo, R. Hoseinnezhad, and R. Mahler, "Robust multi-Bernoulli filtering," *IEEE J. Sel. Topics Signal Process.*, vol. 7, no. 3, pp. 399–409, Jun. 2013.

[14] B. Ristic, B.-T. Vo, B.-N. Vo, and A. Farina, "A tutorial on Bernoulli filters: theory, implementation and applications," *IEEE Trans. Signal Process.*, vol. 61, no. 13, pp. 3406–3430, Jul. 2013.

[15] B. Ristic, *Particle Filters for Random Set Models*. New York: Springer, 2013.

[16] R. Hoseinnezhad, B.-N. Vo, B.-T. Vo, and D. Suter, "Bayesian integration of audio and visual information for multi-target tracking using a CB-MeMBer filter," in *IEEE Int. Con.f Acoust Speech Signal Process.*, Prague, Czech republic, May 22-27, 2011, pp. 2300–2303.

[17] J. Wei and X. Zhang, "Sensor self-organization for mobile multi-target tracking in decentralized wireless sensor networks," in *IEEE Wireless Commun. Networking Conf.*, Sydney, Australia, Apr. 18-21, 2010, pp. 1–6.

[18] B.-N. Vo, B.-T. Vo, N.-T. Pham, and D. Suter, "Joint detection and estimation of multiple objects from image observations," *IEEE Trans. Signal Process.*, vol. 58, no. 10, pp. 5129–5141, Oct. 2010.

[19] R. Hoseinnezhad, B.-N. Vo, and B.-T. Vo, "Visual tracking in background subtracted image sequences via multi-Bernoulli filtering," *IEEE Trans. Signal Process.*, vol. 61, no. 2, pp. 392–397, Jan. 2013.

[20] H. G. Hoang and B.-T. Vo, "Sensor management for multi-target tracking via multi-Bernoulli filtering," *Automatica (in press)*, 2014.

[21] J.L. Williams, "Hybrid poisson and multi-bernoulli filters," in *Int. Conf. Inf. Fusion*, Singapore, Jul. 9-12, 2012, pp. 1103–1110.

[22] I. Arasaratnam and S. Haykin, "Cubature Kalman filters," *IEEE Trans. Automat. Control*, vol. 54, no. 6, pp. 1254–1269, Jun. 2009.

[23] D. Schuhmacher, B.-T. Vo, and B.-N. Vo, "A consistent metric for performance evaluation of multi-object filters," *IEEE Trans. Signal Process.*, vol. 56, no. 8, pp. 3447–3457, Aug. 2008.